

CHAPTER 6: USE OF VERTICAL AND DIAGONAL MEMBERS TO UPGRADE THE STEEL BRACED FRAMES

6.1 ECCENTRICALLY BRACED FRAMES

A retrofitting method for the old designed eccentrically braced frame has been presented in this part. Numerical experimentation has been carried out for the old designed eccentrically braced frame and for their modified versions. According to the current seismic provisions, the behaviour of the old designed eccentric *NCBFs* was not desirable. The contribution of the link in plastic dissipation was minimal even after following the criteria of shear link. Plastic dissipation by the frame, the braces and the beam outside link was undesirably significant. The hysteresis loop was unstable and significant strength degradation was observed.

The structural behaviour has been improved by introducing the retrofitting measures in such a way that the structural interventions and the disruption to the occupants would be minimal. After modification, the maximum plastic dissipation has been contributed by the link portion, as desired. The hysteretic behaviour and the plastic dissipation was improved significantly and the strength degradation was minimised.

6.1.1 Methodology and Design Considerations

In the eccentrically braced frames, most of the plastic dissipation has to be done by the links. In olden days, the eccentricity in the braces was provided for the architectural purpose or the accommodation of openings but various researchers were able to recognise the merits of the eccentric bracing over the concentric bracing. According to Popov (1983), provision of link length (e) to the beam length (L) ratio, e/L less than 0.5 was found to increase the stiffness considerably.

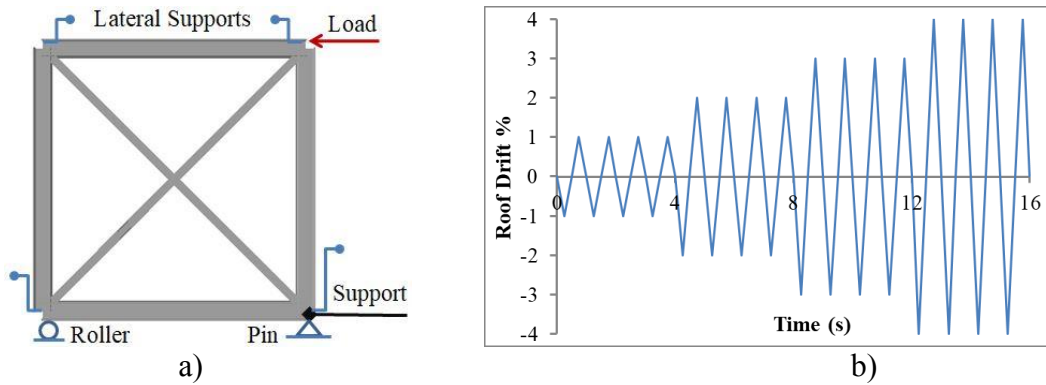


Figure 6.1 a) Experimental arrangement, b) Displacement loading protocol

Sloat (2014) investigated that many of the steel buildings in olden days were equipped with the wide flange chevron braces (*made-up of ASTM-A36 steel; which is equivalent to the JIS-SS 41 steel*). To replicate a generalised conventional eccentrically braced frame; loading arrangement (Figure 6.1.a), loading protocol (Figure 6.1.b), specimen geometry, size of wide flange sections made-up of JIS-SS41 steel (Table 6.1) were referred from a half century old experimental report (Wakabayashi *et. al.* 1980). The contemporary design details (*prior to modifications*) were referred from the works of Popov *et al.* (1983, 1987, 1988). Provisions of JSCE (2009) were also referred.

The height of the frame (h) and the width of the bay (L) were 1.4 m and all the members were rigidly connected. Here, two node cubic beam-elements were used for modelling and numerical analysis in the finite-element based software (Abaqus CAE 2014). Combined hardening and non-linearity (*both material and geometrical*) were included. Quasi-static analysis was performed using displacement control method.

Table 6.1 Member sections and their material properties (Adapted from the experimental results reported by Wakabayashi *et. al.* 1980)

Member	Section (values in mm)	σ_y	σ_u (MPa)	ϵ_p
Beam, Column	100×100×6×8	276	424	0.28
Brace, Diagonals	50×50×6×6	270	409	0.37

Note: σ_y is the yield stress, σ_u is the ultimate stress and ϵ_p is the plastic strain.

The experimental results adapted from the report by Wakabayashi *et al.* (1980) for X-braced frame were validated using numerical simulation (hysteresis loop shown in Figure 6.2) in ABAQUS software (2014) and the results matched with the experimental ones to a good extent. Localised failure became severe after reaching 3% drift in the experiment by Wakabayashi *et al.* (1980) and resulted into serious strength degradation (can be deduced from Figure 6.2).

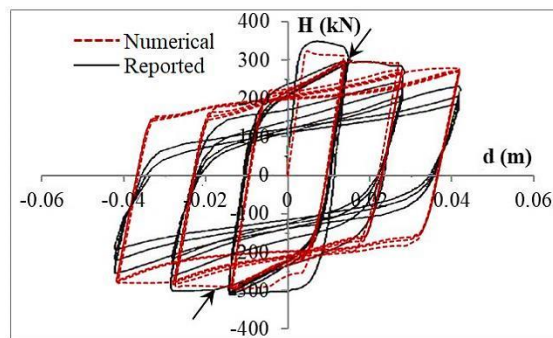


Figure 6.2 Comparison of hysteresis curves for X-braced frame

Analytical and numerical methods have been found incapable of recognising the localised damages, manufacturing deficiencies (*the weak connections resulted from the old method of electrode welding*) and geometrical imperfections; as they depend on various factors that go unacknowledged (Sen *et al.* 2014; Sen *et al.* 2016; Sizemore *et al.* 2017). Numerical simulations were found to be capable of replicating the global behaviour of the braced frame to a good degree (Sen *et al.* 2014; Sizemore 2017). Here, the critical points obtained numerically (*shown by arrows in Figure 6.2*) were in close proximity with the critical points observed in the experimental study.

In the experimental report (Wakabayashi *et al.* 1977, 1980), the individual sections of the frame members and the braces were repeated for all the considered cases irrespective of the bracing configurations. Following that, all those member-sections have been considered here as it is, to form a generalised replica of the conventional eccentrically braced frame (as shown in Figure 6.3.a).

Popov *et al.* (1987) suggested, link length ratio, $a = \frac{e}{(M_p / V_p)} \leq 1.6$ (Equation 5.1)

In Equation 5.1, the plastic shear capacity of the link, $V_p = 0.55.F_y.t_w.d$ (in AISC-2016 seismic provision, $V_p = 0.6.F_y.t_w.(d-2t_f)$) and M_p was the plastic moment capacity. Here, F_y represents the yield stress, ‘ d ’ represents the depth of the section, ‘ t_w ’ represents the thickness of the web and ‘ t_f ’ represents the thickness of the flange.

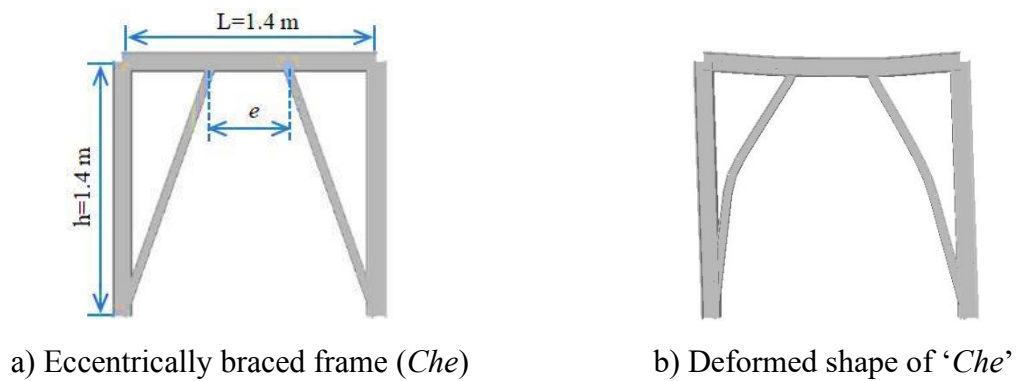


Figure 6.3 Selected eccentrically braced frame

As per Foutch *et al.* (1987) and Roeder (1989) beam panel connecting the braces acted as very short link at weak seismic loads. Short links ($1 < a \leq 1.6$) undergo shear yielding; long links ($a > 2.6$), undergo flexural yielding; and intermediate links ($1.6 < a < 2.6$) experience combination of both shear and flexural yielding (Azad and Topkaya 2017). e/L value for eccentric brace used in present study was 0.35, which was less than 0.5, the value of link length ratio (a) was $1 < a < 1.6$, the braces were compact as per the conclusions of the experimental reports (Wakabayashi *et al.* 1980).

Even after following most of the contemporary design considerations, the link segment of the chevron EBF (*without upgrade*) used here didn't worked as expected by the seismic provision and significant beam deflection was observed (Figure 6.3.b and Figure 6.4.a).

Result of such action was seen in the form of strength degradation (*can be deduced from hysteresis loops shown in Figure 6.4.b*) at the later stages of loading which was similar to the results observed by Popov *et al.* 1988 (*prior to strengthening*).

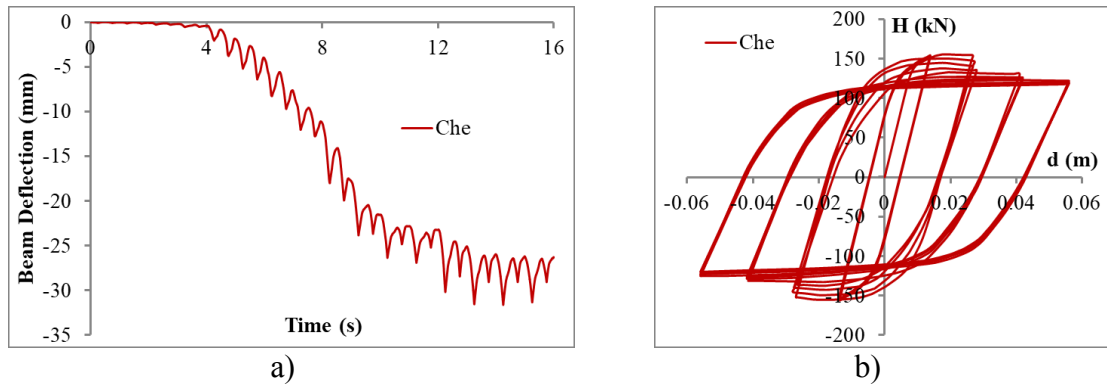


Figure 6.4 a) Central deflection of beam b) Hysteresis loop

Reducing the slenderness of braces by increasing their section (*moment of inertia*) caused adverse effects on the other members (Wakabayashi *et al.* 1977, Narayan *et al.* 2020). So, the braced frame (*Che*) was modified by adding diagonal members at 90° (*Che-D90*), at one-fourth height (*Che-D4*) and at central height (*Che-D0*), as shown in Figure 6.5. Such arrangements introduced nodes in the length of the braces for increasing the buckling load capacity without increasing the section.

The diagonal members (*can be connected easily by following the provisions used for X-brace connections*) were expected to improve the structural behaviour without replacing or dismantling any member and without compromising with the door opening space. The directly welded connections were selected here for the analysis; as used in by other researchers to simulate the behaviour of the conventional frames (Sen 2016). Using Abaqus CAE software, Narayan *et al.* found that the effective length of the buckling members obtained by numerical simulation using beam-elements matched with the experimental measurements to a good extent.

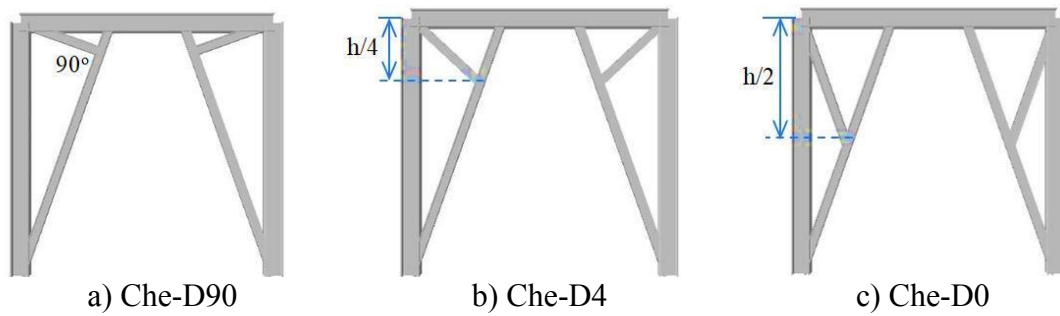


Figure 6.5 Modified eccentric chevron braced frame configurations

6.1.2 Results and Discussion

The modified state of the chevron eccentrically braced frame was analysed for both the monotonic and cyclic loadings. The parameters of the study were the critical load under monotonic loading, hysteretic behaviour (*from which strength degradation can also be recognised*), energy dissipation, beam deflection and link rotation under cyclic loading.

Critical load (P_{cr}) under monotonic loading

Critical load (P_{cr}) of the frame was found using linear perturbation buckling analysis (*Eigen value method*) under both the vertical (V) loading (*at top corners*) and the lateral/horizontal loading (H) separately. Percentage increase from the original state has also been calculated.

Table 6.2 Critical load values of the considered braced frames

Specimen Configuration:		<i>Che</i>	<i>Che-D90</i>	<i>Che-D4</i>	<i>Che-D0</i>
P_{cr} (% increase ↑)	H (in kN)	981.7	1141.1 (16.2 %↑)	1515.9 (54.4 %↑)	2332.3 (137.6 %↑)
	V (in kN)	8999	9372.4 (4.2 %↑)	9304.4 (3.4 %↑)	9267.5 (3.0 %↑)

Here, from the critical load table (Table 6.2), it can be seen that the critical vertical load also increased in the modified state but the lateral load resistance due to the braces was immensely improved. This was a preliminary indication for getting an improved structural behaviour from the braces, so that braces were least involved in the inelastic

activity and allow the link to dissipate energy. Seismic design provisions also suggest to keep the braces of a well-designed eccentrically braced frame in elastic state so that the link does most of the plastic dissipation.

Additional Diagonal Brace Perpendicular to Existing Brace (Che-D90)

In addition to the improvement in lateral load resistance under monotonic loading, improvements under cyclic loading were also observed after employing the additional diagonal braces perpendicular to existing braces connected to the top end corners of the frame. In comparison to the initial state (*Che*), the contribution of the link in the inelastic activity by rotation/shear was significantly improved. After increasing the drift from 3% to 4%, the considerable involvement of the braces in the inelastic activity (see deformed shape in Figure 6.6.a) shadowed the rotation/shear in the link section. It can be seen in Figure 6.6.b that the rotation of the link was disrupted after 12 seconds of loading.

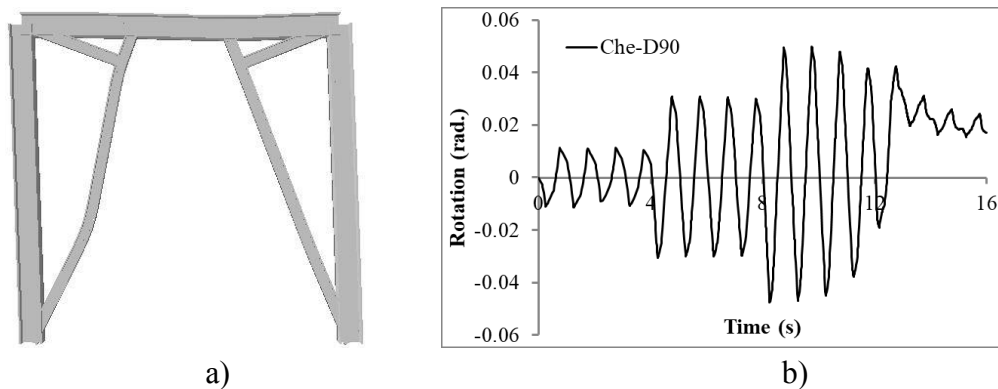


Figure 6.6 a) Deflected shape of Che-D90 configuration b) Rotation of the link

The hysteresis loops shown in Fig. 6.7.a indicate that the '*Che-D90*' braced frame was significantly superior to the that of '*Che*' braced frame. After increasing the roof-drift from 3% to 4% some strength degradation was observed in '*Che-D90*'. The improvement in plastic dissipation (see Figure 6.7.b) was still significant (23% higher); as till 3% drift, the rotation/shear in the link portion was the main source of plastic dissipation.

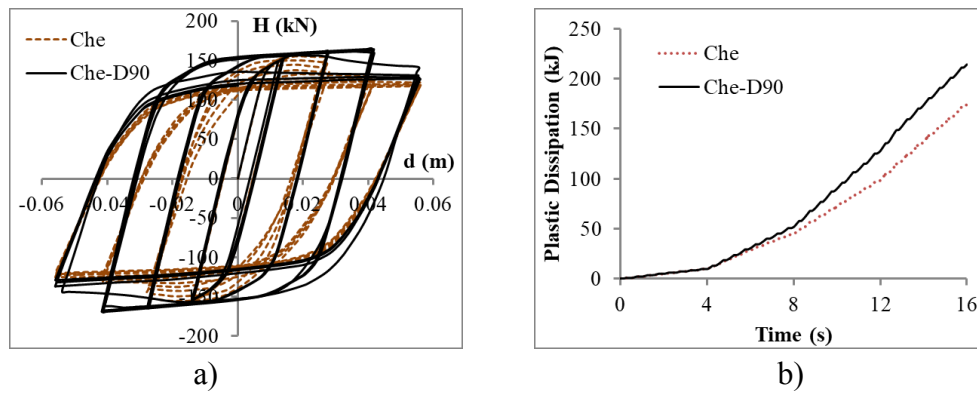


Figure 6.7 a) Hysteresis loop comparison with initial state, b) Plastic dissipation

Additional Diagonal Brace at One-Fourth Height from Top (Che-D4)

On addition of additional diagonal braces connected from the top end corners of the frame to the existing braces at one-fourth height from top, significant improvements in the structural behaviour under cyclic loading were observed. To dissipate energy, the rotation/shear in the link shadowed the effect of the undesirable bending of the beam observed in the unmodified (*Che*) state. Till 12 seconds, rotation/shear in the link portion was the only source of plastic dissipation and after 14 seconds that braces began to involve in the inelastic activity as shown in Figure 6.8.a. But here, the involvement of braces had very less contribution to the inelastic activity. It can be seen in Figure 6.8.b that after 15 seconds, the link portion lost its track of energy dissipation by rotation/shear, which was an effect of the brace deformation at the last stages of the loading.

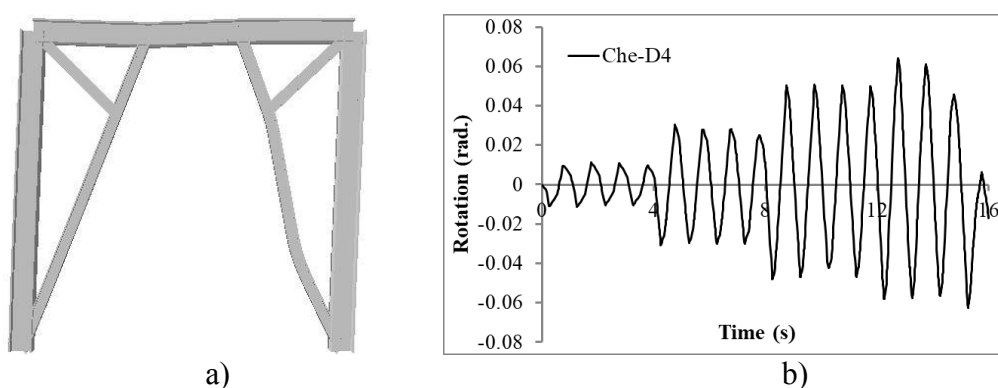


Figure 6.8 a) Deflected shape of Che-D4 configuration b) Rotation of the link

Hysteresis loops shown in Figure 6.9.a were both stable and balanced till 14 seconds of loading, which was within the 8% drift range (4% drift limit). Because of such hysteretic behaviour, this configuration was found to cause maximum plastic dissipation (34% higher) among all the considered configurations (as shown in Figure 6.9.b). Visible strength degradation wasn't observed in the hysteresis loops till 14 seconds. Little strength degradation was observed in the last cycle of the loading.

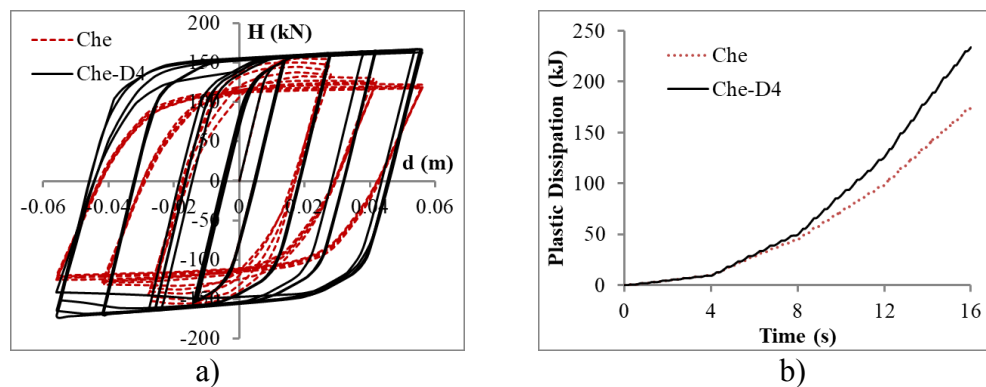


Figure 6.9 a) Hysteresis loop comparison with initial state, b) Plastic dissipation

Additional Diagonal Brace at Central Height (Che-D0)

As observed in Table 6.2, amongst all the considered cases, lateral load resistance was highest in the modified configuration where the additional diagonal braces were connected from the top end corners of the frame to the existing braces at the mid-height of the frame. As observed from Figure 6.10.a, the participation of the link portion in inelastic activity (*plastic dissipation*) by undergoing rotation/shear was very significant at the later stages of loading (*the deformation in the braces was also observed*). As visible from the graph shown in Figure 6.10.b The behaviour of link rotation/shear was most consistent amongst all the considered cases till the end of the loading.

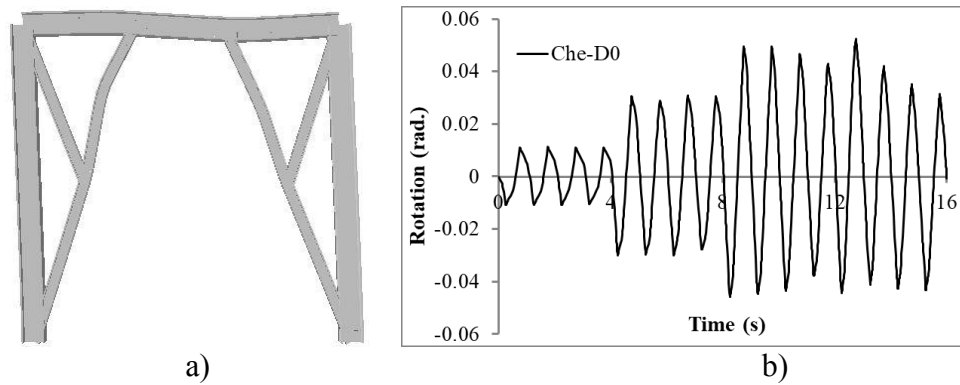


Figure 6.10 a) Deflected shape of Che-D0 configuration b) Rotation of the link

Till 12 seconds, almost all the plastic dissipation was done by the link portion. Even though after increasing the roof-drift from 3% to 4%, the involvement of braces in the inelastic activity increased which resulted in little strength degradation of strength. But as can be seen from Figure 6.11.a, the strength degradation was very minute and the overall hysteresis loop was both balanced and stable. In comparison to the initial configuration (*Che*), this configuration had 32% higher plastic dissipation (see Figure 6.11.b). Looking at the stability of the hysteresis loop, consistency of the shear deformation of the link and the all-round improvement of structural behaviour, this configuration has been considered as the most suitable configuration for retrofitting amongst the considered strategies of upgrade, using the methodologies presented here.

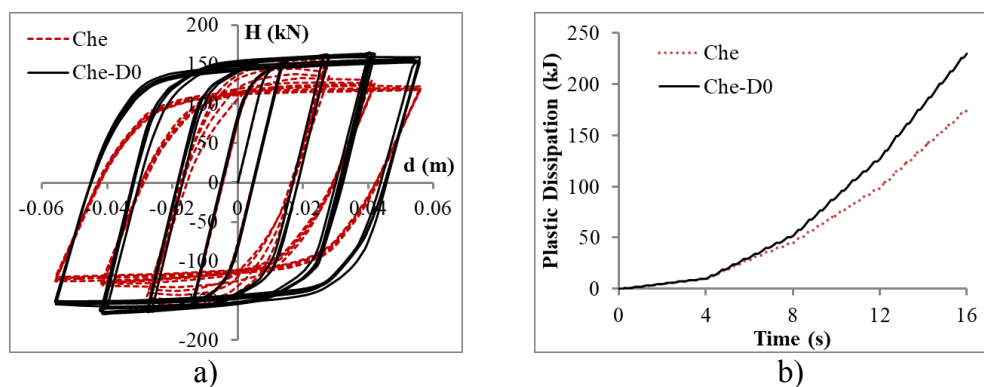


Figure 6.11 a) Hysteresis loop comparison with initial state, b) Plastic dissipation

It was found in the older braced frame state (*Che*) that the deflection of beam was considerably high and the braces were significantly involved in the plastic dissipation. Over that, the tension brace became ineffective due to excessive beam deflection like as generally observed in the concentrically chevron braced frames. Such drawbacks were satisfactorily rectified by the methodologies presented here and a significantly improved structural behaviour (*hysteretic, rotation of link, energy dissipation*) was achieved.

6.2 CONCENTRICALLY BRACED FRAMES

The problem of unbalanced forces acting on the beams in the non-ductile concentric chevron braced frames (*NCBFs*) has been found to become worse when beam deflects excessively at the connections of the braces. It can be concluded from many research articles that the reduction in beam deflection would result into an improved behaviour of the concentrically braced frames under seismic loading. As per the seismic provisions (AISC (2016), JSCE (2009), IS (2007)), to design a new special concentrically braced frame (*SCBF*), stronger beams have been recommended. But in the existing old/conventionally constructed braced frames, replacement of beams with stronger beams (*SCBF based design*) in multi-storied buildings would cause serious disruption (*complete vacation*) to the occupants, would require intensive structural intervention, heavy equipment/machines and very skilled workers (Rai and Goel 2003).

Over that, replacing the braces with stronger braces was not found to be a favourable solution as it was found to cause structural problems in other members and make the structural behaviour of frame more uncertain and less ductile (Wakabayashi *et. al.* 1977, Narayan and Pathak 2020). All these design and construction related constraints were satisfactorily overcome by the very handy and economical strategies suggested here.

The strategies to renovate the NCBFs has been discussed in this part. Two arrangements of upgraded bracing were developed; one configuration was inspired by the combination of the X-braces and Y braces while the other was inspired by the combination of the Zipper braces and Y-braces. Both arrangements resulted into different dual Y-braces (DYB). The outcomes of the renovation were the better hysteretic behaviour, higher plastic energy dissipation and significant reduction in the beam deflection.

6.2.1 Methodology and Specifications of Specimens

The main objectives of any renovation/ retrofitting technique have been to provide an improved structural behaviour to the structure, to avoid the complete replacement and to do it cost-effectively. These considerations were very effectively justified by the work presented here. The initial configuration of chevron brace and the loading configuration (*drift range up-to that applied for failure of the specimen experimented by Wakabayashi 1980*) have been shown in Figure 6.12, respectively.

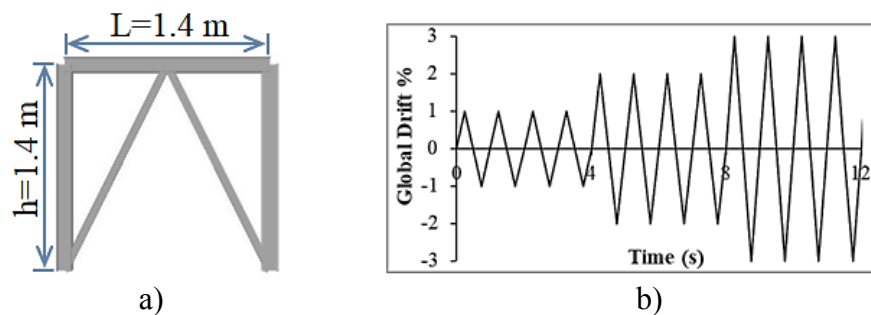


Figure 6.12 a) Chevron braced frame (*Ch*), b) Cyclic Loading protocol

Three configurations were such that the additional diagonals were connected from beam column end connection; perpendicular to the existing braces (Figure 6.13.a), at one-fourth height of frame from top (Figure 6.13.b) or at central height of frame (Figure 6.13.c). In one configuration, vertical members (*emerging from the existing brace at the central height of the frame*) were connected to the beam (Figure 6.13.d).

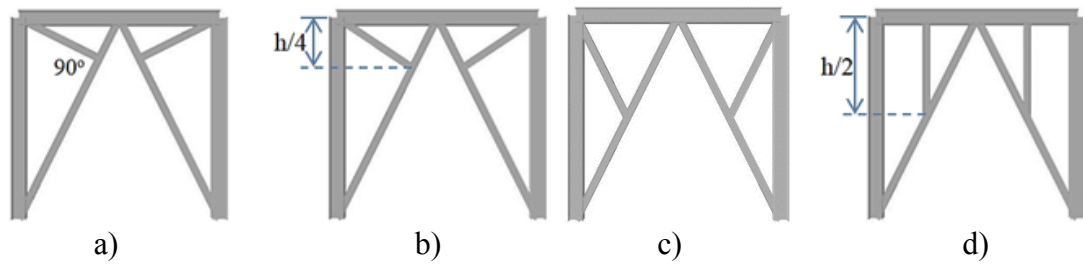


Figure 6.13 Modified chevron braced frame configurations

The design methodologies for the connections have changed drastically over the decades. The gusset plates were of arbitrary size in olden braced frame constructions. Many of the braced frames were directly welded. The structural steel manufactured nowadays wouldn't represent the steel used in olden constructions as it varies in strength and properties in comparison to the one manufactured in olden days. So, to replicate a generalized old braced frame, the material properties and the member sections were referred from an old experimental report (Wakabayashi *et. al.* 1980).

Here, the design provisions from various countries were referred (JSCE, 2009, IS:800, 2007 and ANSI/AISC 341-16, 2016) along with the contemporary reports about the olden construction practices (Wakabayashi *et. al.* 1977, 1980). Specification of the member sections adapted from Wakabayashi *et. al.* (1980) has been provided in the Table 6.1 and other numerical analysis related details were same as provided in previous part 6.1.1.

6.2.2 Results and Discussion

The results of the numerical analysis of the selected chevron braced frames were obtained in the form hysteresis loops, plastic dissipation time-history graphs, specimen deformed shapes and beam deflections. In the unmodified state of the chevron braced frame (*Ch*), the undesirable spikes were observed in the hysteresis curves for the few initial loading cycles (shown in Figure 6.14.a), which made the hysteresis curve unstable unbalanced. The energy dissipation for that configuration has been shown in Figure 6.14.b.

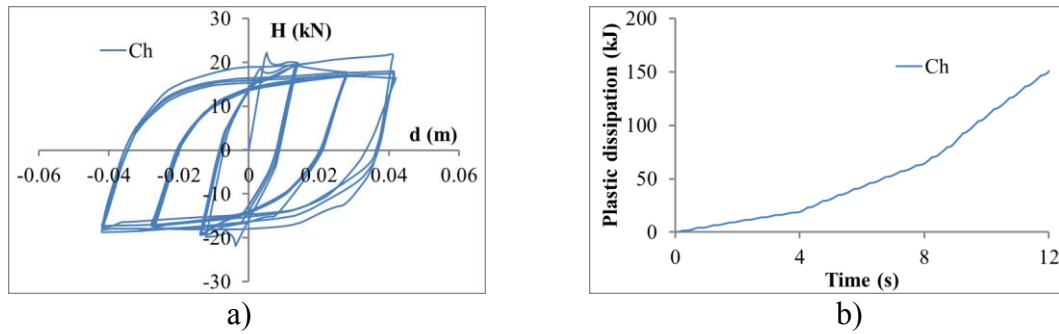


Figure 6.14 a) Hysteresis loop for ‘Ch’ braced frame, b) Energy dissipation

The deformation profile of the unmodified chevron braced frame has been shown in Figure 6.15.a and the time history plot of the beam deflection has been shown in Figure 6.15.b. The deflection of beam at 3% roof drift has been found close to 45 mm.

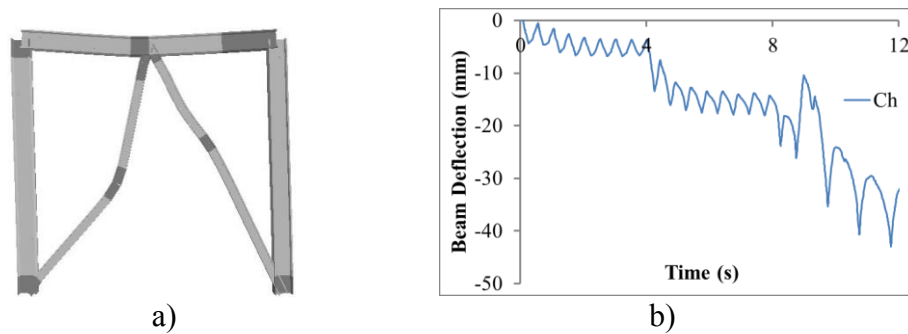


Figure 6.15 a) Deformation profile of chevron braced (Ch) frame (*yielding zones shown by dark shades*), b) beam deflection

It can be seen that the inelastic action of beam was also predominant along with the inelastic action of the braces, which has not been recommended. As the lateral drift was increased, the deflection of beam also increased with time. To avoid problems caused by beam deflection, various modifications were done to upgrade the chevron braced frames.

Member from beam column joint perpendicular to the brace (Ch-D90)

In this modification, diagonals were connected from the beam-column connection end, perpendicular to the existing brace. The deformed shape at a particular time has been shown in the Figure 6.16.a. Inelastic activity was profound only in the lower part of braces

(as the effective length was considerably high). The deflection of beam was very much reduced from maximum of close to 45 mm to less than 30 mm (as shown in Figure 6.16.b) but the inelastic activity in the beam at various points of times was significant, so one purpose of reducing beam deflection was satisfied but the drawback of beam deflection was not completely rectified in this case.

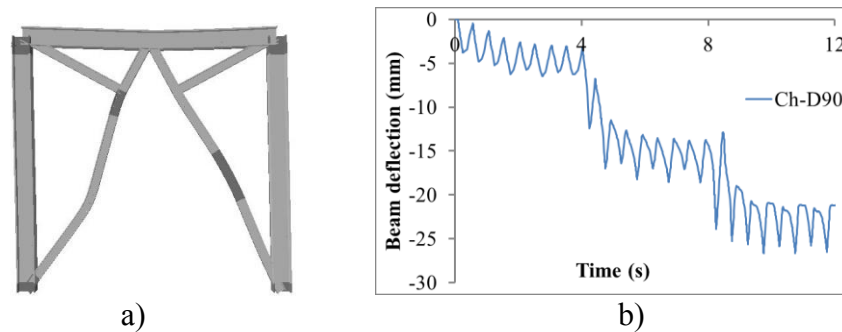


Figure 6.16 a) Deformed shape of *Ch-D90* braced frame, b) beam deflection

The hysteretic behaviour improved (see Figure 6.17.a) in comparison to the unmodified state. But the improvements were not significant as the energy dissipation (see Figure 6.17.b) improved minutely and the inelastic activity in the beam was still significant.

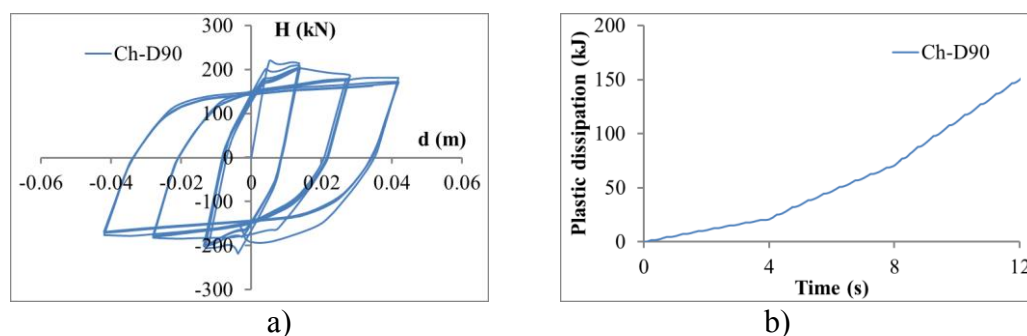


Figure 6.17 a) Hysteresis loop for *Ch-D90* braced frame, b) Energy dissipation

Additional brace from beam column joint to brace at 1/4th height from top (Ch-D4h)

In the existing chevron braced frame, additional diagonals from the beam-column connection end to the existing brace were connected rigidly at a vertical height of one-fourth of the total story height. The deformed shape has been shown in the Figure 6.18.a.

Inelastic activity was profound only in the lower part of braces (*as the effective length was considerably high*). The deflection of beam was considerably reduced from close to 45 mm to less than 30 mm (shown in Figure 6.18.b) but out of all the considered modified braced frames, this configuration had maximum inelastic activity in the beam.

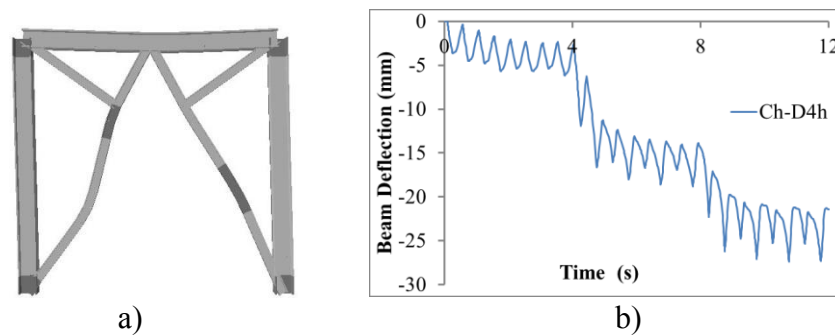


Figure 6.18 a) Deformed shape of *Ch-D4h* braced frame, b) beam deflection

The inelastic activity in the beam was reduced in comparison to the unmodified case. The hysteresis loop became more balanced (see Figure 6.19.a) but the improvements were not significant and the energy dissipation (see Figure 6.19.b) was also not that improved and the beam was still contributing in the inelastic activity along with the braces.

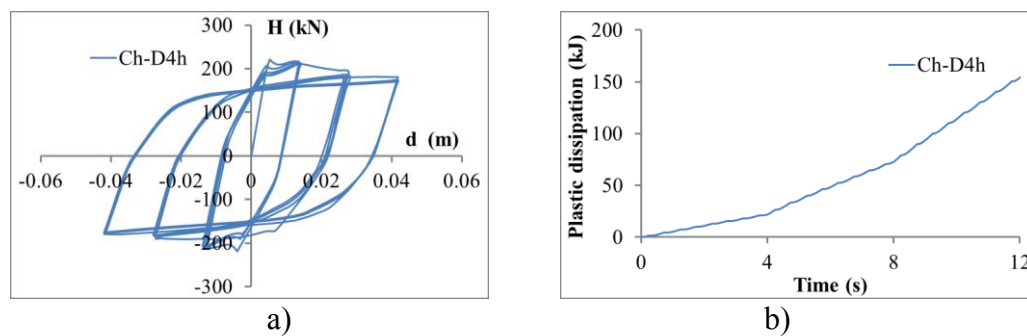


Figure 6.19 a) Hysteresis loop for *Ch-D4h* braced frame, b) Energy dissipation

Diagonal member from the centre of the brace (Ch-D)

For the modified configuration having an additional diagonal member connected from the beam column connection to the brace at the central height of the frame, the results were very much acceptable and reformed in comparison to the unmodified configuration.

The sudden peaks/spikes observed in the hysteresis loops of the unmodified chevron braced configuration in the initial stages of loading were diminished, the hysteresis loops were more balanced and stable (see Figure 6.20.a). The energy dissipation also found to be improved considerably (see Figure 6.20.b).

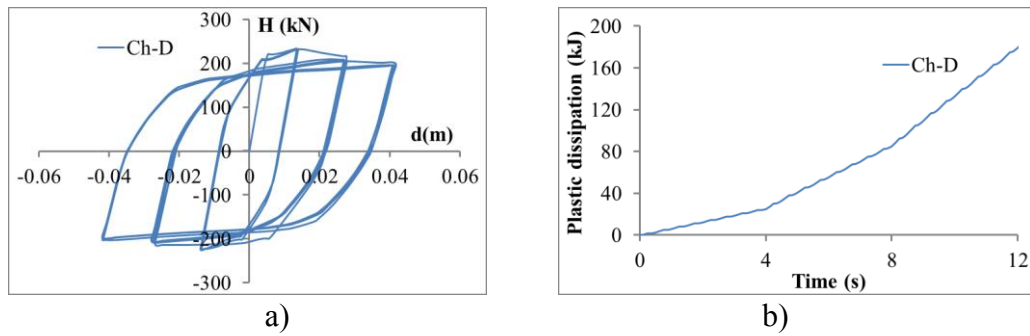


Figure 6.20 a) Hysteresis loop for *Ch-D* braced frame, b) Energy dissipation

The inelastic activity was predominant in the braces (*desirable*). The deformed shape has been shown in the Figure 6.21.a. Inelastic activity was profound only in the upper part of braces. As the effective length was reduced considerably it can be expected to improve both the strength and the ductility. This configuration has been found to be one of the most acceptable configurations amongst all the considered configurations as it satisfied both the purposes of reducing the beam deflection (*from close to 45 mm to less than 25 mm; as shown in Figure 6.21.b*) and reducing the inelastic activity in the beam section, which in turn would improve the inelastic activity in the braces.

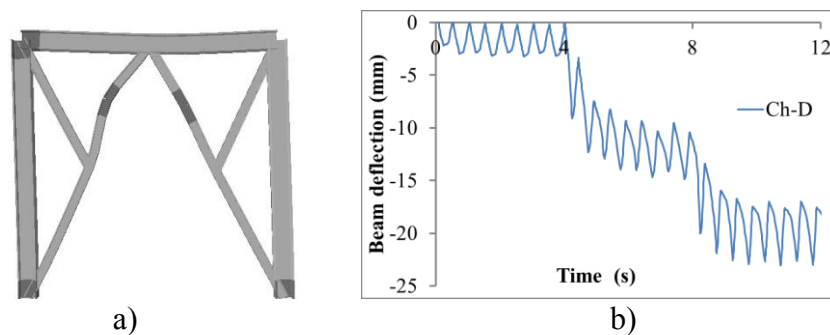


Figure 6.21 a) Deformed shape of *Ch-D* braced frame, b) beam deflection

Vertical member from the centre of the brace (Ch-V)

In the existing chevron braced frame, an additional diagonal brace was connected from the brace at the central height of the frame perpendicular to the beam. The sudden decreasing peaks/spikes observed in the hysteresis loops of the unmodified chevron braced configuration in the initial loading stages were diminished, the hysteresis loops were more balanced and stable (see Figure 6.22.a). The energy dissipation also improved significantly (see Figure 6.22.b). This configuration improved the behaviour of the braced frame significantly as the inelastic activity in the beam was minimised and the braces were found to be the most predominant members in dissipating the energy as expected.

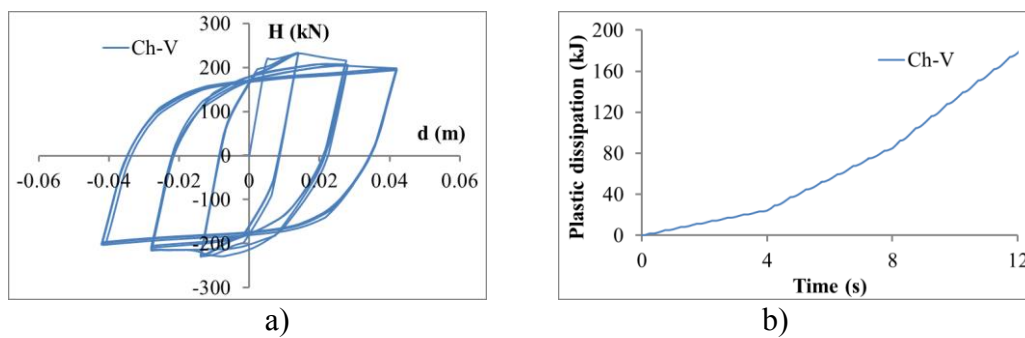


Figure 6.22 a) Hysteresis loop for *Ch-V* braced frame, b) Energy dissipation

The deformed shape at a particular time has been shown in the Figure 6.23.a. This configuration experienced least inelastic activity in the beam (*desirable*) as the two additional members acted as supports. Inelastic activity was profound only in the upper part of the braces and as the effective length was reduced considerably it has been expected to have better the strength and the ductility. This configuration was also one of the most acceptable configurations amongst all the considered configurations as it satisfied both the purposes of reducing the beam deflection (*from close to 45 mm to less than 30 mm; as shown in Figure 6.22.b*) and reducing the inelastic activity in the beam section, which in turn improved the inelastic activity in the braces.

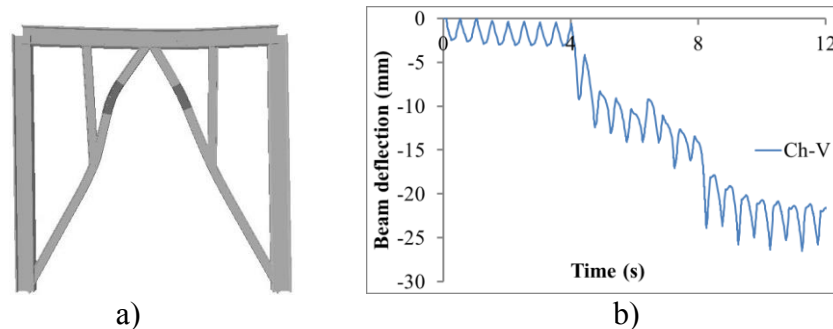


Figure 6.23 a) Deformed shape of *Ch-V* braced frame, b) beam deflection

In the unmodified braced frame, it was found that in third set of the incremental displacement loading, the beam deflection was highly abrupt as it changed from 10 mm to 35 mm on the load reversal. In all the retrofitted cases, no such high abrupt changes in the beam deflection were observed. In the braced frames where additional members were connected to the centre of the brace, the beam deflections were quite gentle. The members connected at the centre of the brace were found to better improve the behaviour of the old chevron braced frame under cyclic loading in comparison to the other cases.

Strength and Plastic dissipation

Not only the behaviour under repeated loading was improved but the strength/resistance to the lateral load was also improved significantly. The critical loads (P_{cr}) under lateral/horizontal (H) and vertical loads (V) have been provided in the Table 6.3. Compared to the critical load for the initial state, Ch , critical loads were also close to 2.5 times higher in the cases where the additional members were connected to the centre of the existing braces. This indicated toward the improvement in the strength along with the ductility of those modified braced frame cases.

Table 6.3 Critical load values of the considered braced frames

Specimen Configuration		Ch	$Ch-D90$	$Ch-D4h$	$Ch-D$	$Ch-V$
P_{cr}	H (in MN)	1.02	1.43	1.60	2.48	2.46
	V (in MN)	10.6	10.8	10.8	10.9	10.7

Where the addition members were connected at the centre of the existing brace, the plastic dissipation was close to 1.5 time that of the initial unmodified configuration. The improvement in the structural behaviour can also be understood from the improvement in the plastic dissipation of the conventional frame, as shown in Figure 6.24.

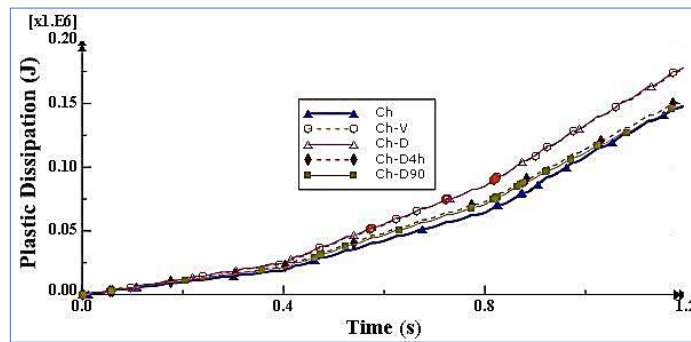


Figure 6.24 Time history plot for plastic dissipation in various configurations

The additional steel take-off required to upgrade the chevron braced frames (*both eccentric and concentric*) using the renovation strategies proposed in this chapter was close to just 9% of the total steel used in the initial chevron braced frame.

6.3 CONCLUDING REMARKS

The EBFs and CBFs were upgraded by adding vertical or diagonal members (*resulting into dual Y-braced frames*) attached to the existing braces. The eccentrically braced frames were upgraded to a very good extent. The structural behaviour of the CBFs was also improved significantly but in these cases, the hysteresis curves showed initial buckling peaks and little strength degradation at the later stages of loading. Conclusions have been discussed elaborately in the last chapter, ‘SUMMARY AND CONCLUSIONS’.